ICMIEE22-166

NUMERICAL STUDY OF HEAT TRANSFER FROM A HEATED FLAT SURFACE UNDER CO- AND COUNTER-ROTATING SWIRLING COAXIAL TURBULENT IMPINGING JETS

Farhana Afroz[1], *Muhammad A.R. Sharif*[1,*]
[1] Aerospace Engineering and Mechanics Department, The University of Alabama, Tuscaloosa, Alabama, USA

ABSTRACT
Swirling coaxial impinging jet heat transfer has been investigated recently by many researchers. Swirling motion in the impinging jet has been found to either enhance or diminish the heat transfer depending on the combination of the flow parameters. The present paper investigates the flow dynamics and thermal transport processes from an isothermal hot surface under turbulent coaxial impinging jets with co- and counter-rotating swirling motion. The ratio of the inner to the outer diameter of the coaxial jet is 0.35, and the Reynolds number based on the outer jet diameter is 25,000, while the coaxial jet velocity ratio (defined as the inner and outer jet mean axial velocity ratio) is kept as unity in the current study. The jet inlet swirl strength is varied as 0, 0.44, and 1.25 with co- and counter-rotating swirl directions for the inner and outer jets, and the jet exit to target distance is varied as 0.5 and 2 times the outer jet diameter. The ANSYS Fluent commercial code is used for numerical computations. The computational model uses a highly refined mesh and is validated against published experimental and numerical data. The SST k-ω turbulence model is used for the computations which show good agreement between the predicted and published data. The streamlines, isotherms, and swirl velocity contours depict the effect of the co- and counter-rotating jet swirl on heat transport. It is found that the overall heat transfer is affected positively (enhancement) or negatively (reduction) by the swirl motion. The direction of the swirl (co- or counter-rotating) has an insignificant effect except at higher separation distances and higher swirl strengths.

Keywords: Numerical simulation, heat transfer, impinging jet, coaxial jet, swirling jet, turbulent jet.

1. Introduction

There are many practical applications of coaxial jets in aerospace propulsion, combustion process, cooling systems, and jet pumps; among others. A thin-walled tube is inserted inside a coaxial outer tube to construct a coaxial jet nozzle. The inner tube carries fluid for the inner jet while the annular space between the inner and outer tube carries the fluid for the outer jet. The two jet fluids with different flow properties interact outside the jet pipe within the free jet region. The influential parameters in the coaxial swirling jet flow, which control the jet impingement heat transfer behavior are; the average jet velocities of the inner jet (U_i) and the outer jet (U_o), the inner jet diameter (D_i) and the outer jet diameter (D_o), the jet exit to impingement surface separation distance (h), the swirl strength of the inner and outer jets (Sw), and the Reynolds number (Re) for the inner and outer jets. The jet velocity ratio λ (= U_i / U_o) and jet diameter ratio $d = D_i/D_O$ are also important parameters in this context.

Many studies have been conducted to comprehend the free coaxial jet flows under varying velocity ratios, λ, smaller and larger than unity. Ko and Kwan [1] and Kwan and Ko [2] investigated free coaxial jet flow and demonstrated that a very complex flow field exists downstream of the jet exit. Three different flow regimes were identified, which they termed (*i*) the initial, (*ii*) intermediate, and (*iii*) full merging zones. Warda et al. [3] reported that inner and outer jet mixing is better when the velocity ratio λ is < 1. Segalinia and Talamelli [4] experimentally showed that the inner mixing region dominates the jet flow when λ < 0.75 while the outer mixing region drives the jet flow for λ > 1. In contrast, the coaxial impinging jet (non-swirling) heat transfer has been undertaken only by a few researchers. Celik and Eren [5] experimentally conducted coaxial jet impingement heat transfer with a relatively lower diameter ratio of D_i/D_O = 0.105 and demonstrated that the heat transfer is enhanced compared to that for a circular single jet. Celik and Bettenhausen [6] performed numerical studies of coaxial jet impingement heat transfer at various Reynolds numbers with varying diameter ratios to reveal heat transfer enhancements in comparison to a single round jet. Bijarchi and Kowsary [7] recently investigated coaxial jet impingement heat transfer and achieved more heat flux uniformity at the impingement plate. Swirling circular impinging jets were numerically investigated by Salman et al.[8] and Sharif [9]. They observed that the enhancement or reduction of heat transfer in a single swirling impinging jet depends on the combination of the separation distance and swirl strength. The subject of swirling coaxial jet impingement heat transfer has not been noticeably investigated yet. Recently, Afroz and Sharif [10] numerically investigated turbulent swirling coaxial jet impingement heat transfer. They observed that the spreading and mixing of the jet and resulting heat transfer are noticeably affected due to the swirl motion.

The present study numerically investigates turbulent swirling coaxial jet impingement heat transfer from an isothermal plane surface. In addition to the velocity ratio (λ), diameter ratio (d), and the Reynolds number (Re); the non-dimensional jet exit-to-impingement surface separation distance H (= h/D_o), and the swirl strength Sw (the azimuthal momentum/the axial momentum), are two other important flow and geometric variables in the study of swirling coaxial jet impingement heat transfer. The values of required parameters are taken as d = 0.35; λ =

* Corresponding author. Tel.: +1(205)348-8052
E-mail address: msharif@eng.ua.edu

1.0; Re = 25,000; H = 0.5 and 2; and Sw = 0, 0.44, and 1.25 in this study. The swirling motion of the inner and outer jet can be specified as co-rotating and counter-rotating. Thus, one of the main objectives of this study is to investigate the effect of co-rotating and counter-rotating swirls on the heat transfer from the hot impingement surface.

2. NUMERICAL MODEL

The flow configuration is axisymmetric. As such, an axial (X-direction, along the jet axis) and radial (Y-direction, along the impingement surface) plane of the flow domain is shown in Fig.1. The domain is ($H + 10D_o$) long in the axial direction and $15D_o$ wide in the radial direction. This size of the domain is sufficient to exclude the end effects on the model computations, as evidenced in previous works of other researchers. The Ansys Fluent CFD code is used for all computations in this study.

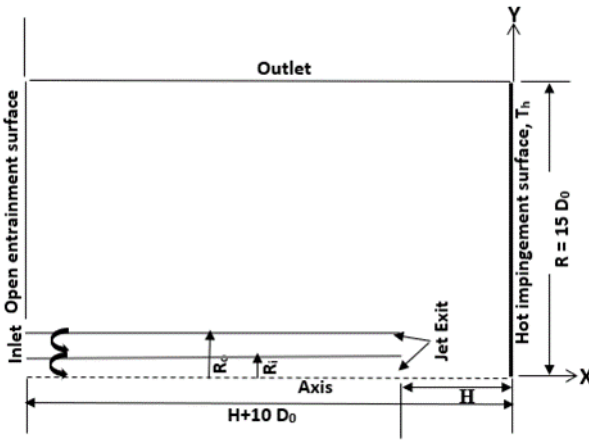

FIG. 1 Schematic diagram of coaxial swirling impinging jet and sample mesh

Conservation of mass, momentum, and energy, with constant fluid properties are the governing equations for the present problem. For the axisymmetric swirling flow, the velocity component in the azimuthal direction is taken as a passive scalar in the Fluent code.

The governing partial differential equations are integrated over the generated finite volume cells to obtain a set of linear algebraic equations. These equations are solved sequentially and iteratively to produce the normalized residuals below 10^{-6} for all equations. Calculation monitoring is also done by plotting the total heat flux at the impingement plate with iterations until it levels off.

The mesh for the domain is chosen after a systematic mesh refinement study. A mesh with 46,439 cells is deemed to produce mesh independent solution. The model is validated against the published numerical and experimental data. Based on the validation study, the SST k-ω turbulence model, as implemented in the Fluent code, is used for all computations in this study.

The isothermal (T_h = 315 K) impingement surface is the right boundary of the flow domain where no-slip conditions are imposed. Adiabatic no-slip conditions are also imposed on the walls of the coaxial jet. Uniform axial velocities are imposed at the inner and outer jet inlets where the temperature is maintained at T_c = 300 K. At the outlet boundary, pressure outlet boundary condition is applied. At the entrainment boundary, pressure inlet condition is imposed. The swirl motion is specified as a solid body rotation at the jet inlet. For the co-rotating case, the swirl motion is counter-clockwise for both inner and outer jets whereas the swirl direction for the inner jet is counterclockwise and that for the outer jet is clockwise for the counter-rotating case.

3. Results

3.1 Co-Rotating Coaxial Swirling Impinging Jet

Some representative results for the co-rotating coaxial impinging jet are presented in Figs. 2 and 3 showing the flow streamlines, the contours of the swirl velocity component, and the contours of the temperature for representative cases with H = 2 and 4, respectively, at Re = 25,000, d = 0.35, and λ = 1.5. These contour plots demonstrate that the flow patterns and isotherms are significantly affected as the swirl strength is increased from the non-swirling condition. The penetration of the imposed swirl up to the impingement surface is observed from the contours of the swirl velocity. The streamlines and contours of the swirl velocity change noticeably at higher swirl strength of 1.25. The formation of a small recirculation bubble at the right lower corner of the flow domain at a lower separation distance (H = 2) is observed, due to which a radially downstream shift of the main jet flow away from the axis of the domain occurs. The isotherms are thickened in that region because of this flow characteristic which affects the overall heat transfer process. Some effects of the swirl on the streamlines, contours of the swirl velocity, and isotherms at a higher distance of separation (H = 4) are observed in Figs. 2 and 3. At the higher swirl of Sw = 1.25, the main jet flow is deflected away from the domain axis and the thermal boundary layer is thickened near the axis region.

3.2 Co-and Counter-Rotating Swirling Coaxial Impinging Jet

The streamlines, isotherms, and contours of the swirl velocity for H = 0.5 is shown in Fig. 4. The negative sign in front of Sw indicates a counter-rotating swirl while the positive sign implies a co-rotating swirl. Thus, the upper part of Fig. 4 shows the contours for the counter-rotating swirling case and the lower part shows that for the co-rotating case both for swirl strength Sw = 1.25. The contours do not show any distinguishable differences in features between the co- and counter-rotating swirling cases. The impinging jet and wall jet development is almost similar. A bubble separates the inner jet from the outer jet. The impingement locations for the inner and outer jets are separated due to this bubble development. The thermal boundary layer is slightly thicker near the impingement locations for the counter-swirling case (Sw = −1.25) than that for the co-swirling case. The implication is that the local peak Nusselt number at the impingement location is lower for the counter-rotating

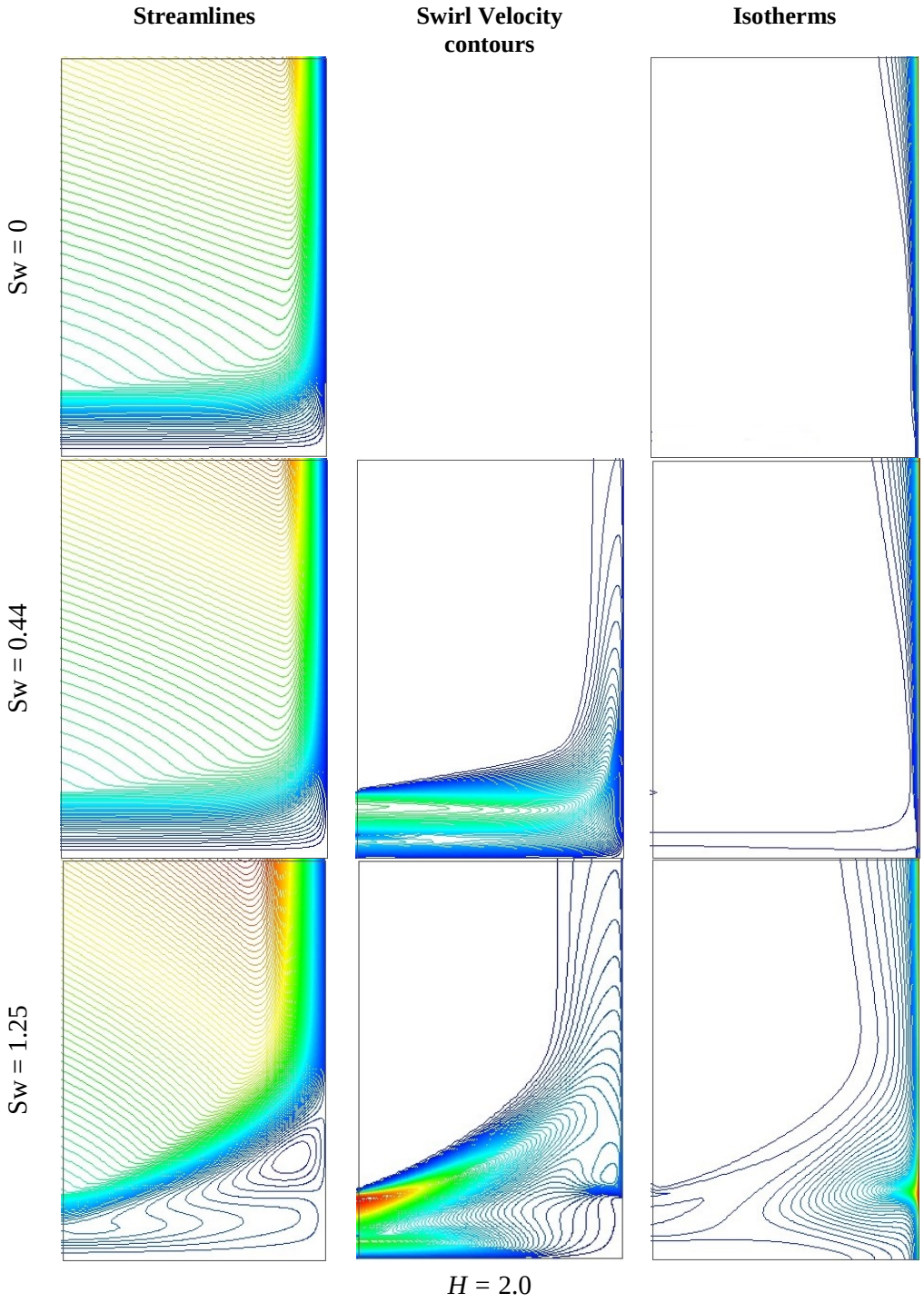

FIG. 2. Contour plots of the stream function, swirl velocity magnitude, and temperature distribution in the flow domain for different swirl strengths; Re = 25,000, d = 0.35, λ = 1.5, and H = 0.5, H = 2.0.

case than that for the co-rotating case. The swirl motion penetrates the entire gap from the jet outlet to the impingement plane incorporating a strong swirl motion in the impingement region and the wall jet region. The swirl velocity component contributes to the radial velocity component and modifies the resultant velocity tangential to the free surface in the impingement and wall jet region, which affects the convective heat transfer from the surface positively or negatively.

The heat transfer behavior from the impingement surface is analyzed by extracting the distribution of the local Nusselt number at the surface along a radial line, from which the average surface Nusselt number is

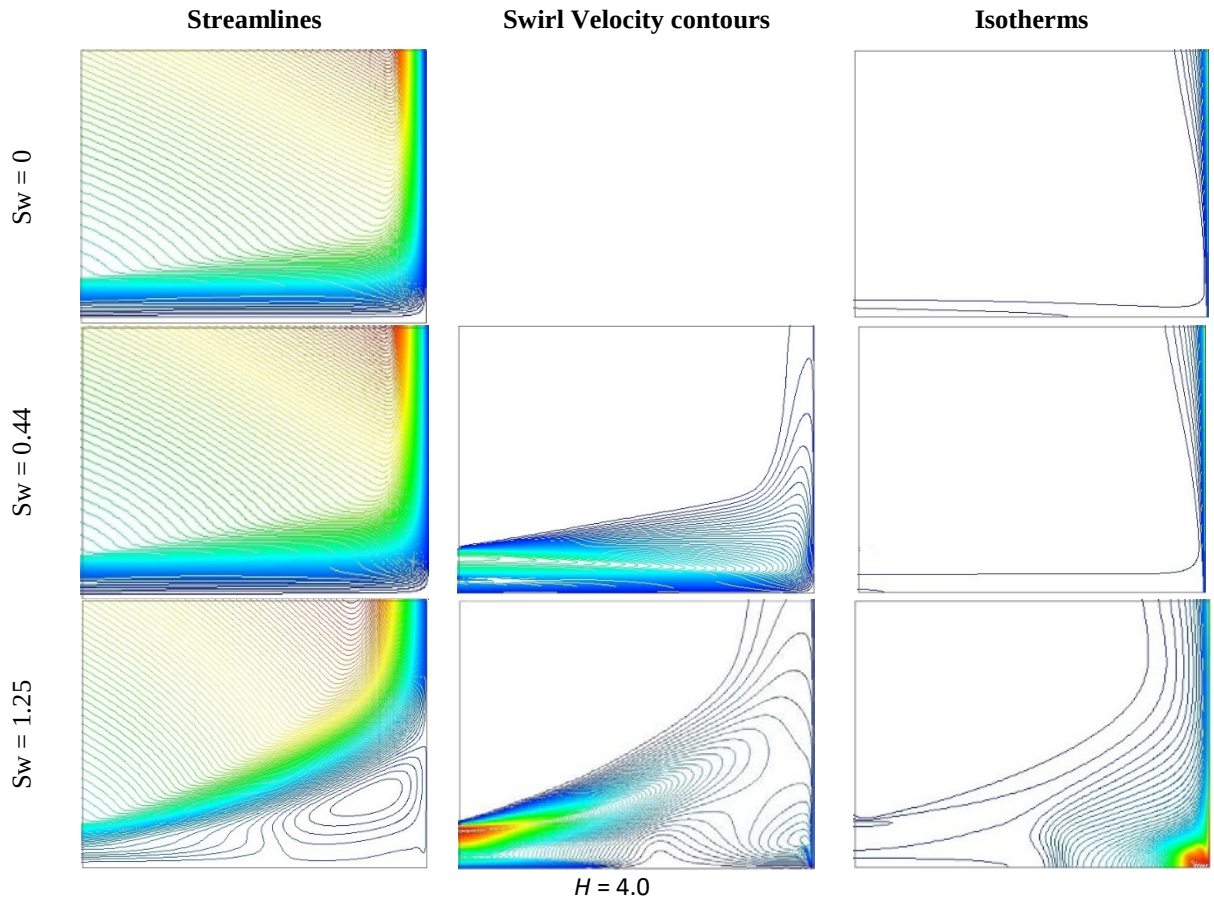

FIG. 3. Contour plots of the stream function, swirl velocity magnitude, temperature distribution in the flow domain for different swirl strengths; Re = 25,000, d = 0.35, λ = 1.5, and H = 4.0.

calculated. The plot of the local Nusselt number is presented in Fig. 5 for the counter- and co-rotating jets with Sw = ±1.25 at velocity ratios 1.0 and 1.5 for a separation distance of H = 0.5. The local Nusselt numbers fluctuate with maximum and minimum values. The secondary maximum Nusselt number occurs at the location where the main jet stream impinges on the surface. At λ = 1.0, there is a significant difference in the Nusselt number distribution between the counter and co-rotating cases. At the higher λ = 1.5, the Nusselt number distribution is almost the same for the counter and co-rotating cases.

The average surface Nusselt number for the different combinations of the flow and geometric parameters is plotted in Fig. 6 against the swirl strength. It is seen that the overall heat transfer is enhanced at a low distance of separation (H = 0.5) as the swirl strength is increased while at a higher distance separation (H = 2) the heat transfer initially diminishes at low swirl strength (Sw = 0.44) but then enhances at high swirl strength (Sw = 1.25); in comparison to the no-swirling case. The percent change of the average Nusselt number in comparison to the no-swirling case for the various cases is presented in Table 1 to better comprehend the overall heat transfer process. It is evident from the plot in Fig. 6 and Table 1 data that, the co-rotating and counter-rotating swirl configuration has an insignificant effect on the overall heat transfer from the surface except at higher swirling strength and low separation distance (Sw = 1.25, H = 0.5).

4. CONCLUSIONS

Heat transfer from a heated flat plate under turbulent, coaxial, co-rotating, and counter-rotating swirling impinging jets is numerically investigated for two jet-to-target separation distances (H = 0.5 and 2) and three swirl strengths including the non-swirling case (Sw = 0, 0.44, and 1.25). The objective was to investigate the effect of co-rotating and counter-rotating swirl motion on the overall heat transfer from the impingement plate. It is found that, while the overall heat transfer is affected positively (enhancement) or negatively (reduction) by the swirl motion, the swirl direction (co- or counter-rotating swirl) has an insignificant effect except at higher separation distance and swirl strength. At a low separation distance, heat transfer is enhanced with increasing swirl strength in comparison to the no-swirling case. At a higher separation distance, the overall heat transfer diminishes at low swirl strength (Sw = 0.44) but enhances at larger swirl strength (Sw = 1.25).

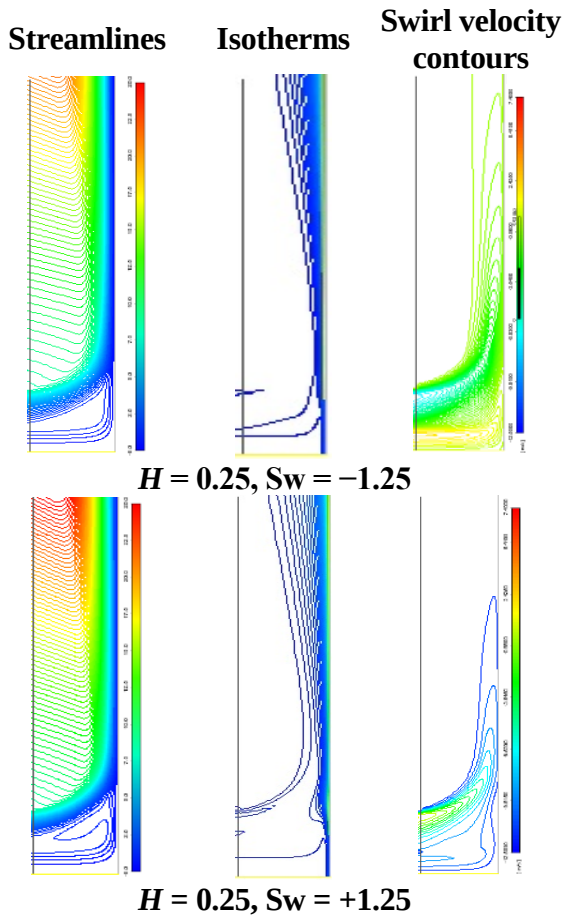

FIG. 4 Streamlines, isotherms, and swirl velocity contour on the radial-axial plane at co- and counter-rotating swirl conditions.

5. References

[1] N. Ko, A. Kwan, The initial region of subsonic coaxial jets, Journal of Fluid Mechanics. 73 (2) (1976) 305-332.

[2] A. Kwan, N. Ko, The initial region of subsonic coaxial jets. Part 2, Journal of Fluid Mechanics. 82 (2) (1977) 273-287.

[3] H.A. Warda, S.Z. Kassab, K.A. Elshorbagy, E.A. Elsaadawy, An experimental investigation of the near-field region of free turbulent round central and annular jets, Flow Measurement and Instrumentation. 10 (1) (1999) 1-14.

[4] A. Segalini, A. Talamelli, Experimental analysis of dominant instabilities in coaxial jets, Physics of Fluids. 23 (2) (2011) 024103.

[5] N. Celik, H. Eren, Heat transfer due to impinging coaxial jets and the jets' fluid flow characteristics, Experimental Thermal and Fluid Science. 33 (4) (2009) 715-727.

[6] N. Celik, D.W. Bettenhausen, Numerical investigation of the coaxial impinging jets with various diameter ratios, Journal of Enhanced Heat Transfer. 19 (2) (2012).

[7] M.A. Bijarchi, F. Kowsary, Inverse optimization design of an impinging coaxial jet to achieve heat flux uniformity over the target object, Applied Thermal Engineering. 132 (2018) 128-139.

[8] S.D. Salman, A.A.H. Kadhum, M.S. Takriff, A.B. Mohamad, Experimental and numerical investigations of heat transfer characteristics for impinging swirl flow, Advances in Mechanical Engineering. 6 (2014) 631081.

[9] M.A.R. Sharif, Numerical investigation of round turbulent swirling jet impingement heat transfer from a hot surface, Computational Thermal Sciences: An International Journal. 8 (6) (2016).

[10] F. Afroz, M.A.R. Sharif, Heat Transfer From a Heated Flat Surface Due to Swirling Coaxial Turbulent Jet Impingement, Journal.of Thermal Science and Engineering Applications. 13(2) (2021) 021009 (13 pages).

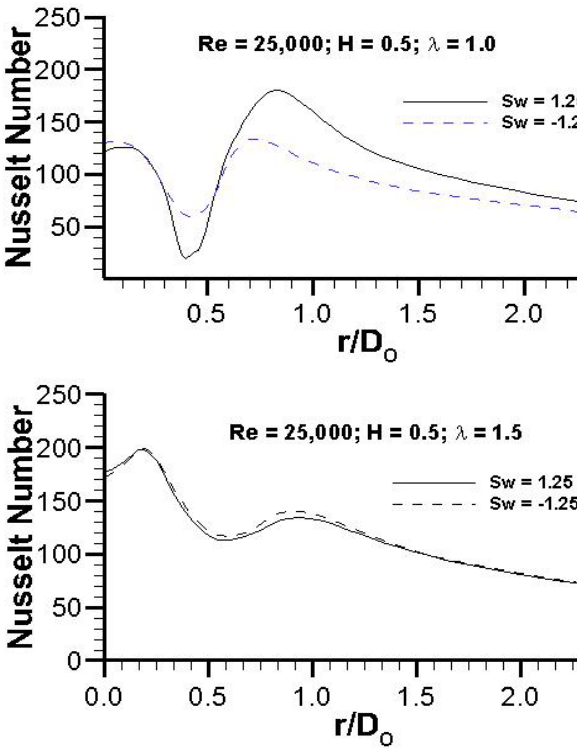

Fig. 5 Local Nusselt number distribution in the radial direction on the impingement surface.

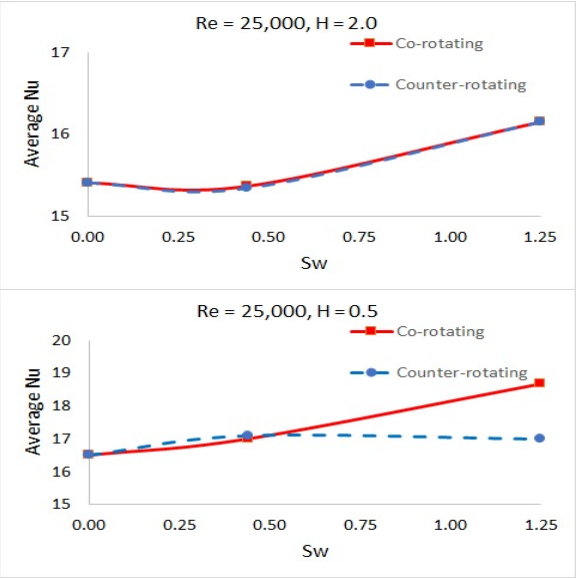

FIG. 6 Average Nusselt number comparison with increasing swirl strength

Table 1 Percent change of the average Nusselt number from non-swirling jet

Sw		H = 0.5		H = 2	
		Average Nu	**Percent change**	**Average Nu**	**Percent change**
0.44	Counter-rotating	17.10	3.67	15.34	-0.43
	Co-rotating	17.00	3.06	15.37	-0.25
1.25	Counter-rotating	17.00	3.06	16.16	4.86
	Co-rotating	18.68	9.90	16.15	4.81

NOMENCLATURE

d : diameter ratio, D_i/D_o
D_i : inner jet diameter, m
D_o : outer jet diameter, m
h : dimensional distance from jet exit to surface, m
H : non-dimensional separation distance, h/D_o
Re : Reynolds number
Sw : Swirl strength
U_i : average inlet velocity at the inner jet, ms^{-1}
U_o : average inlet velocity at the outer jet, ms^{-1}
λ : velocity ratio, U_i/U_o